The EMBO Journal Vol. 20 No. 8 pp. 1875–1887, 2001

The *Arabidopsis thaliana* ABC transporter *At*MRP5 controls root development and stomata movement

Nicola Gaedeke[1], Markus Klein[2], Uener Kolukisaoglu[3], Cyrille Forestier[4], Axel Müller[5], Mark Ansorge[1], Dirk Becker[6], Yasmine Mamnun[7], Karl Kuchler[7], Burkhard Schulz[3], Bernd Mueller-Roeber[1,8] and Enrico Martinoia[2,9]

[1]Max-Planck-Institut für Molekulare Pflanzenphysiologie (MPI-MP), D-14424 Potsdam, [3]Botanisches Institut II, Universität zu Köln, Max-Delbrück-Laboratorium in der Max-Planck-Gesellschaft, Carl-von-Linné-Weg 10, D-50829 Köln, [5]Lehrstuhl für Pflanzenphysiologie, Ruhr-Universität, D-44780 Bochum and [6]Institut für Botanik 1, Universität Würzburg, Julius-von-Sachs Platz 2, D-97082 Würzburg, Germany, [2]Institut de Botanique, Laboratoire de Physiologie Végétale, Université de Neuchâtel, Rue Emile Argand 13, CH-2007 Neuchâtel, Switzerland, [4]CEA-CEN Cadarache, DEVM-LEMS, BP 1, F-13108 St Paul Lez Durance, France and [7]Department of Molecular Genetics, University of Vienna, Dr Bohr-Gasse 9/2, A-1030 Vienna, Austria

[8]Present address: Universität Potsdam, Institut für Biochemie und Biologie, Abteilung Molekularbiologie, Karl-Liebknecht-Strasse 25, Haus 20, D-14476 Golm/Potsdam, Germany

[9]Corresponding author
e-mail: enrico.martinoia@bota.unine.ch

N.Gaedeke and M.Klein contributed equally to this work

In the present study, we investigated a new member of the ABC transporter superfamily of *Arabidopsis thaliana*, *At*MRP5. *AtMRP5* encodes a 167 kDa protein and exhibits low glutathione conjugate and glucuronide conjugate transport activity. Promotor–β-glucuronidase fusion constructs showed that *AtMRP5* is expressed mainly in the vascular bundle and in the epidermis, especially guard cells. Using reverse genetics, we identified a plant with a T-DNA insertion in *AtMRP5* (mrp5-1). mrp5-1 exhibited decreased root growth and increased lateral root formation. Auxin levels in the roots of mrp5-1 plants were increased. This observation may indicate that *At*MRP5 works as an auxin conjugate transporter or that mutant plants are affected in ion uptake, which may lead to changes in auxin concentrations. Experiments on epidermal strips showed that in contrast to wild type, the sulfonylurea glibenclamide had no effect on stomatal opening in mrp5-1 plants. This result strongly suggests that *At*MRP5 may also function as an ion channel regulator.

Keywords: ABC transporter/*Arabidopsis*/*At*MRP5/root development/stomata

Introduction

The ABC transporter superfamily is a very large protein family, which can be found in all organisms from bacteria to plants and man (Henikoff *et al*., 1997). The discovery of ABC transporters in animals is closely linked to their capacity to confer multidrug resistance (MDR) to cancer cells by overexpressing members of this gene family (Gottesman and Pastan, 1993). In eukaryotic organisms, ABC transporters are implicated in the excretion (extracellular or intracellular into the vacuoles) of potentially toxic compounds such as alkaloids, organic anions and heavy metals. In addition, certain ABC transporters may exhibit or modulate ion channel activity (Anderson *et al*., 1991; Szczypka *et al*., 1994; Higgins, 1995; Bryan and Aguilar-Bryan, 1999).

The first ABC transporter isolated from plants was an MDR-like gene from *Arabidopsis thaliana* (*At*PGP1; Dudler and Hertig, 1992). Further experiments showed that *At*PGP1 is localized in the plasma membrane and involved in hypocotyl elongation in light-grown seedlings (Sidler *et al*., 1998). The second observation indicating that ABC transporters occurred in plants was that glutathione conjugate (GS-X) transport into vacuoles depended directly on MgATP hydrolysis and was independent of the electrochemical potential created by the vacuolar proton pumps (Martinoia *et al*., 1993). Recent results indicate that, as in animals, ion fluxes may be mediated or controlled by ABC transporters. Leonhardt *et al*. (1997, 1999) showed that stomata opening in *Comelina* guard cells can be induced by treatment with the sulfonylurea glibenclamide and other drugs affecting ion conductance controlled by the sulfonylurea receptor (SUR) and the cystic fibrosis transmembrane regulator (CFTR).

*Hs*MRP1 (Cole *et al*., 1992) was the first protein characterized as a functional GS-X pump (Leier *et al*., 1994; Müller *et al*., 1994). It was shown subsequently that *Hs*MRP2 and 3 also exhibit GS-X transport activity. However, in addition to GS-X, these transporters accept other organic anions such as glucuronide conjugates or sulfated substances. The different MRPs exhibit marked kinetic differences. It has also been shown that they are localized in different tissues and/or different membranes, suggesting specific functions for different isoforms (König *et al*., 1999).

In animals, the transport of natural substrates by multidrug resistance-associated proteins (MRPs) such as GS-Xs, bile acids or glucuronides has been established. In contrast, only few plant-borne substrates for MRPs have been identified in plants, such as chlorophyll catabolites or glucuronides (Hinder *et al*., 1996; Klein *et al*., 2000).

The observation that *Hs*MRP1 and the MRP homologue yeast cadmium factor 1 (*Sc*YCF1) (Szczypka *et al*., 1994) exhibit GS-X transport activity (Li *et al*., 1996; Tommasini *et al*., 1996) as well as high sequence similarity resulted in the isolation and functional characterization of three MRP-like genes from *Arabidopsis* (Lu *et al*., 1997, 1998; Tommasini *et al*., 1998). Functional complementation in yeast and transport studies revealed

their ability to act as GS-X pumps. *At*MRP2 and *At*MRP3, unlike *At*MRP1, also catalyse the transport of chlorophyll catabolites. Very recently, it was shown that at least *At*MRP2 accepts glucuronides as an additional substrate class (Liu *et al*., 2001).

Sequence analysis of entries in genomic and expressed sequence tag (EST) databases reveals 14 members of the MRP subfamily in *A.thaliana*. The fact that a large number of MRP-like proteins are present in plants raises the question of what their specific roles may be. A powerful tool in investigating development and physiology of plants is the analysis of mutant phenotypes. It is possible to search for loss-of-function mutants in order to study gene function in intact plants. The problems of redundancy of physiological pathways including gene families and interaction between different genes and gene products may thus be solved using a mutant analysis strategy. Reverse genetic procedures have been established to perform PCR screens on large pooled populations of *Arabidopsis* transformants carrying T-DNA insertions. This approach allows the relatively rapid isolation of knockout mutants for any gene of interest (Azpiroz-Leehan and Feldmann, 1997). Plants that are homozygous for the T-DNA insertion can be used for phenotypic, physiological and genetic analyses (Winkler and Feldmann, 1998).

In this study, we present the cloning and functional characterization of a new member of the MRP family in *A.thaliana*, *At*MRP5. In order to understand its role in plant metabolism, we have investigated its expression using transgenic plants harbouring promotor–β-glucuronidase (GUS) fusions. Furthermore, we analysed a T-DNA insertion mutant that was identified by reverse genetics.

Results

AtMRP5 encodes an ABC transporter protein

Using EST database analysis and cDNA library screening, we were able to identify a 5.1 kb cDNA that encodes a novel ABC transporter protein (*At*MRP5) from *A.thaliana*. Additional sequence information corresponding to the 5′-untranslated region (5′-UTR) of the *AtMRP5* mRNA was obtained by RACE-PCR. The *AtMRP5* cDNA contains an open reading frame (ORF) which encodes a protein that spans 1514 amino acids with a predicted mol. wt of 167 kDa (Figure 1A). An in-frame stop codon upstream of the start ATG indicated that the complete *At*MRP5-coding region was present on the cDNA.

The alignment of the *AtMRP5* cDNA with BAC sequence F20D22.11 (DDBJ/EMBL/GenBank accession No. AC002411) allowed us to deduce the genomic organization of the *AtMRP5* gene as well as its intron–exon structure (Figure 1B). The gene maps on chromosome 1 of *A.thaliana* and consists of 11 exons and 10 introns, with the first intron of 192 bp located within the 5′-UTR. The two ATP-binding cassettes of *At*MRP5 are similar to those conserved in the ABC superfamily proteins (Higgins, 1992), each consisting of a domain of ~200 amino acids and comprising the ATP-binding motifs Walker A (GXXGXG) and Walker B (T/IYLLD) (Walker *et al*., 1982) and the ABC signature ([LIVMFY]-S-[SG]-G-X(3)-[RKA]-[LIVMYA]-X-[LIVMF]-[AG]) (Higgins, 1992). The N-terminal ATP-binding cassette of *At*MRP5 contains two well-conserved A and B Walker motifs with a typical ABC signature, whereas the C-terminal ATP-binding cassette contains a degenerated Walker B motif (ILVLD).

A phylogenetic analysis of *AtMRP5* (Figure 2) reveals that this gene forms a subcluster with *AtMRP3–AtMRP9*, while *AtMRP1* and *2* cluster in a separate branch (Martinoia *et al*., 2000). *AtMRP3*, which at present is the only biochemically characterized *AtMRP* gene of this subgroup (Tommasini *et al*., 1997, 1998), exhibits 50% identity and 71% similarity to *AtMRP5*. Interestingly, a phylogenetic tree indicates that the *At*MRP5 subcluster is at least as closely related to the SUR and CFTR as to human MRPs and yeast YCF1. This is not the case for *At*MRP1 and *At*MRP2.

AtMRP5 is an organic anion transporter

It has been shown that YCF1, which confers resistance to cadmium, also functions as a GS-X transporter in yeast (Li *et al*., 1996; Tommasini *et al*., 1996). In order to investigate whether *At*MRP5 is also a GS-X pump, we cloned the full-length *AtMRP5* cDNA into a yeast expression vector and transformed the recombinant plasmid (pN-*At*MRP5) into the cadmium-hypersensitive yeast strain DTY168, in which the *YCF1* coding sequence had been deleted (Szczypka *et al*., 1994). *At*MRP5 could partially complement GS-X transport activity in Δ*ycf1* (not shown). The transport activities were typical for ABC transporters: (i) inhibition by vanadate; and (ii) insensitivity to bafilomycin A1, a specific inhibitor of V-type H^+-ATPases, and NH_4Cl, which disrupts the pH gradient generated by proton pumps. These findings indicate that the transport mechanism is independent of the electrochemical potential generated by proton pumps. It should be mentioned that independent transformants exhibited different transport activities, and in some preparations no transport activity could be observed. Yeast *ycf1* mutants transformed with *AtMRP5* did not restore cadmium tolerance, confirming that in spite of the rather broad substrate specificity of investigated MRPs, the affinity towards a given substrate may vary among these transporters (König *et al*., 1999).

ATP-dependent uptake of oestradiol-17-(β-D-glucuronide) ($E_2$17G) and a rye flavonoid glucuronide was reported for vacuoles from rye and barley (Klein *et al*., 1998, 2000). Yeasts exhibit a low transport activity for glucuronides, but up to now yeast glucuronide transporters have not been identified. We introduced the construct pN-*At*MRP5 into the YYA4 yeast strain exhibiting a reduced glucuronide transport activity. The yeast mutant transformed with *AtMRP5* was able to transport $E_2$17G when compared with the empty vector control. The transport revealed typical characteristics of an ABC-type transporter protein as described above for GS-Xs (Table I). Reduced glutathione, oxidized glutathione and dinitrobenzene glutathione (DNB-GS) had no effect on $E_2$17G uptake. However, the *At*MRP5-dependent transport activity of $E_2$17G was severely influenced by other organic anions such as oestradiol-3-sulfate, the natural flavone-glu-curonide luteolin-7-*O*-diglucuronide-4′-*O*-glucuronide, glycocholate and the sulfonylurea glibenclamide. For unknown reasons and as observed for GS-X transport activity, transport rates

A

```
aatcttcttc cactactttg cacaatcttt aatcgatcca accaataaat tttgcatttt      60
ttttcgttgg cgaatgaagg attagagaga aacagaagaa attgttaatt tttttcttgt     120
tgattttaat taaagagaag agagatctct cttctcgatt gctctcaaga acccaagtga     180
cgtctggttt cagctgattt gtttcttctc attctctatc ttcttctctg ggaaatatcg     240
attttgatct attaagagct ggctacgagc tttgggatgt ggtgagatgc ttgttctatc     300
tcgaacaatc cgccggttgt tgattttaaa caaactctct atcacaaatc tttcccgatc     360

ATGGATTTTA TTGAGATCTC GTTGATCTTT CGAGAGCATT TGCCACTACT GGAACTATGT     420
M  D  F  I   E  I  S   L  I  F   R  E  H  L   P  L  L   E  L  C
      20
SVIINLLLFL VFLFAVSARQ ILVCVRRGRD RLSKDDTVSA SNLSLEREVN HVSVGFGFNL      80
SLLCCLYVLG VQVLVLVYDG VKVRREVSDW FVLCFPASQS LAWFVLSFLV LHLKYKSSEK
LPFLVRIWWF LAFSICLCTM YVDGRRLAIE GWSRCSSHVV ANLAVTPALG FLCFLAWRGV     200
SGIQVTRSSS DLQEPLLVEE EAACLKVTPY STAGLVSLIT LSWLDPLLSA GSKRPLELKD
IPLLAPRDRA KSSYKVLKSN WKRCKSENPS KPPSLARAIM KSFWKEAACN AVFAGLNTLV     320
SYVGPYLISY FVDYLGGKEI FPHEGYVLAG IFFTSKLIET VTTRQWYMGV DILGMHVRSA
LTAMVYRKGL KLSSIAKQNH TSGEIVNYMA VDVQRIGDYS WYLHDIWMLP MQIVLALAIL     440
YKSVGIAAVA TLVATIISIL VTIPLAKVQE DYQDKLMTAK DERMRKTSEC LRNMRVLKLQ
AWEDRYRVRL EEMREEEYGW LRKALYSQAF VTFIFWSSPI FVAAVTFATS IFLGTQLTAG     560
GVLSALATFR ILQEPLRNFP DLVSMMAQTK VSLDRISGFL QEEELQEDAT VVIPRGLSNI
AIEIKDGVFC WDPFSSRPTL SGIQMKVEKG MRVAVCGTVG SGKSSFISCI LGEIPKISGE     680
VRICGTTGYV SQSAWIQSGN IEENILFGSP MEKTKYKNVI QACSLKKDIE LFSHGDQTII
GERGINLSGG QKQRVQLARA LYQDADIYLL DDPFSALDAH TGSDLFRDYI LSALAEKTVV     800
FVTHQVEFLP AADLILVLKE GRIIQSGKYD DLLQAGTDFK ALVSAHHEAI EAMDIPSPSS
EDSDENPIRD SLVLHNPKSD VFENDIETLA KEVQEGGSAS DLKAIKEKKK KAKRSRKKQL     920
VQEEERVKGK VSMKVYLSYM GAAYKGALIP LIILAQAAFQ FLQIASNWWM AWANPQTEGD
ESKVDPTLLL IVYTALAFGS SVFIFVRAAL VATFGLAAAQ KLFLNMLRSV FRAPMSFFDS    1040
TPAGRILNRV SIDQSVVDLD IPFRLGGFAS TTIQLCGIVA VMTNVTWQVF LLVVPVAVAC
FWMQKYYMAS SRELVRIVSI QKSPIIHLFG ESIAGAATIR GFGQEKRFIK RNLYLLDCFV    1160
RPFFCSIAAI EWLCLRMELL STLVFAFCMV LLVSFPHGTI DPSMAGLAVT YGLNLNGRLS
RWILSFCKLE NKIISIERIY QYSQIVGEAP AIIEDFRPPS SWPATGTIEL VDVKVRYAEN    1280
LPTVLHGVSC VFPGGKKIGI VGRTGSGKST LIQALFRLIE PTAGKITIDN IDISQIGLHD
LRSRLGIIPQ DPTLFEGTIR ANLDPLEEHS DDKIWEALDK SQLGDVVRGK DLKLDSPVLE    1400
NGDNWSVGQR QLVSLGRALL KQAKILVLDE ATASVDTATD NLIQKIIRTE FEDCTVCTIA
HRIPTVIDSD LVLVLSDGRV AEFDTPARLL EDKSSMFLKL VTEYSSRSTG IPEL          1514
```

B

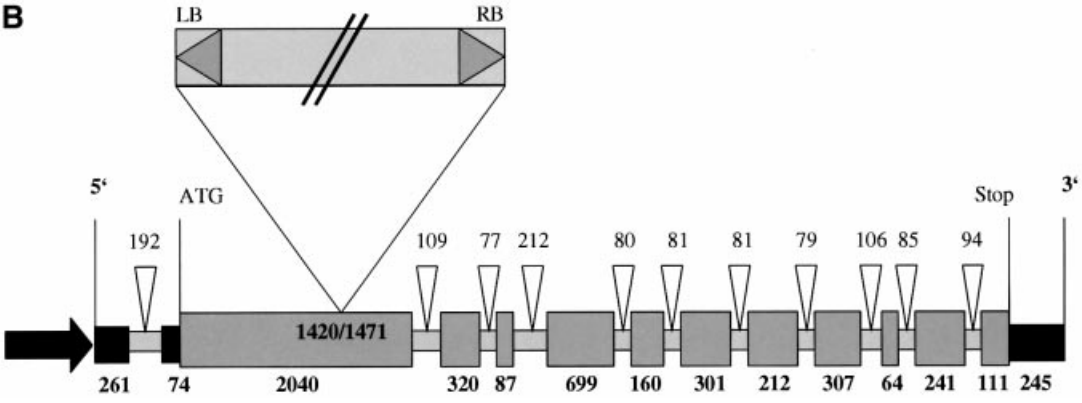

Fig. 1. Sequence and genomic structure of *AtMRP5*. (**A**) The predicted *At*MRP5 protein sequence. Lower case letters of the gene sequence indicate the 5′-non-translated sequence. Putative transmembrane-spanning domains identified using the TMpred program (Hofmann and Stoffel, 1993) are underlined; the Walker motifs A and B, as well as motif C, are represented as small grey boxes. The methionine, incorrectly annotated in gene F20D22.11 (DDBJ/EMBL/GenBank accession No. AC002411) as being the first amino acid, is boxed. (**B**) Genomic organization of the *AtMRP5* gene as deduced from the cDNA and a corresponding genomic sequence located on BAC F20D22. The promoter (arrow), as well as the 5′- and 3′-UTRs are shown as black boxes; exons are presented as dark grey, introns as light grey boxes. Exon and intron sizes are given in bold and standard letters, respectively. The insertion site and the orientation of the T-DNA in the *mrp5-1* mutant is indicated.

of the complemented YYA4 strain differed greatly from one preparation to another.

AtMRP5 is expressed mainly in vascular tissues and epidermis

In order to understand the physiological function of *At*MRP5, we analysed its expression pattern by RNA gel blot analysis and conducted promoter studies using transgenic plants expressing *At*MRP5 promoter–GUS fusion constructs. In RNA blot as well as in RT–PCR experiments, *AtMRP5* mRNA accumulation was detected in seedlings, flowers, roots, siliques and leaves (data not shown). For the promoter–GUS fusion experiments, we isolated two different promoter fragments of *AtMRP5*, of

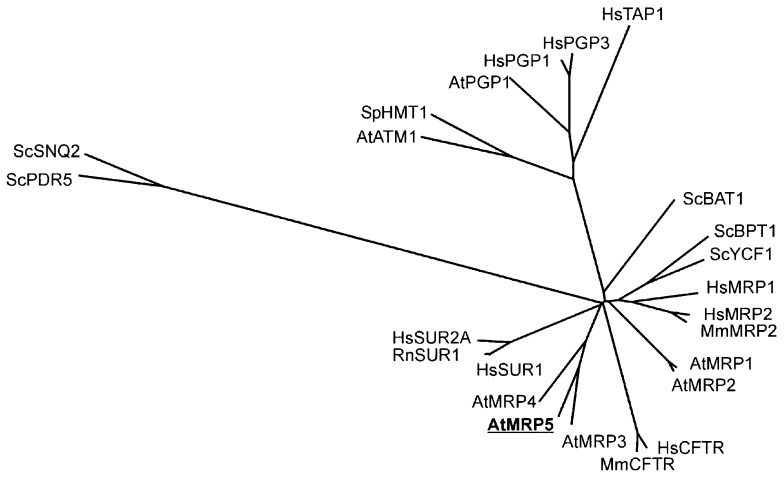

Fig. 2. Phylogenetic comparison of representative members of the ABC transporter superfamily from yeast, mammals and *Arabidopsis*. The unrooted phylogenetic tree shown is based on a multiple alignment of 24 full-length polypeptide sequences of ABC transporters produced by the CLUSTAL program in the DNASTAR DNA analysis software package. Distance matrix was calculated with a PAM matrix and the tree was calculated with the NEIGHBOR-JOINING program using the phylogenetic analysis program package PHYLIP (version 3.57c; University of Washington, 1995). Bootstrap analysis (100 replicates) confirmed the structure of the tree, whereas basal nodes showed low values (<50%) due to the close branching of individual clusters. All other values were >80%, most of them 100% (U.Kolukisaoglu, data not shown). Protein sequences used in this analysis were: *At*MRP1 (AF008124), *At*MRP2 (AAC16268), *At*MRP3 (U96250), *At*MRP4 (AJ002584), *At*MRP5 (this study), *At*PGP1 (X61370), *At*ATM1 (AF287697), *Hs*MRP1 (P33527), *Hs*MRP2 (NP000383), *Hs*CFTR (M28668), *Hs*PGP1 (P08183), *Hs*PGP3 (P21439), *Hs*TAP1 (Q03518), *Hs*SUR1 (Q09428), *Hs*SUR2A (AAC16057), *Mm*MRP2 (AAF61707), *Mm*CFTR (P26361), *Rn*SUR1 (L40624), *Sc*YCF1 (P39109), *Sc*BPT1 (P14772), *Sc*BAT1 (P32386), *Sc*PDR5 (L19922), *Sc*SNQ2 (P32568) and *Sp*HMT1 (Q02592). The two letters preceding the protein names describe the organisms from which the sequences were derived: At, *Arabidopsis thaliana*; Hs, *Homo sapiens*; Mm, *Mus musculus*; Rn, *Rattus norvegicus*; Sc, *Saccharomyces cerevisiae*; Sp, *Schizosaccharomyces pombe*.

1.8 and 3 kb length. Both promoter fragments comprised the complete 5′-UTR of the corresponding cDNA including the nucleotides encoding the first six amino acids of the *At*MRP5 protein. The two *AtMRP5* promoter fragments were joined to the GUS-coding region. More than six lines were analysed for each promoter–reporter gene construct. No significant difference in expression pattern was detected between the lines carrying the two promoters, indicating that all *cis*-elements relevant for *At*MRP5 expression were present on the shorter 1.8 kb promoter fragment.

GUS gene expression driven by the *AtMRP5* promoter was tested in seedlings and mature plants by staining with 5-bromo-4-chloro-3-indolyl-β-D-glucuronic acid (X-Gluc; Figure 3). In seedlings grown on sterile culture medium, strong GUS staining was observed in cotyledons and roots (Figure 3A and G). In roots of seedlings and mature plants, GUS activity was restricted to the central cylinder and was absent from the root cortex and the root tip (Figure 3G).

In mature leaves, the *AtMRP5* gene appeared to be expressed most strongly in the vascular tissue of leaves. Almost all vascular strands of lower and higher order veins were stained in strongly expressing lines (Figure 3B and C). GUS staining in weakly expressing lines was most prominent in vascular anastomoses (data not shown). GUS staining in vascular tissue was not restricted to individual cells, but was seen in almost every cell (with the exception of xylem cells) of the vascular strand (Figure 3C). Considerable GUS activity was also detected in leaf epidermal cells including mature guard cells of leaves and flower petals (Figure 3C–E). In some cases, weak staining was seen in parenchyma cells. In anthers, high GUS activity was concentrated along the central vascular strand of the filament and in the tissue connecting the pollen sacs (Figure 3F). Interestingly, intense GUS staining was also visible at the silique attachment site of the pedicel, as seen in Figure 3H, indicating that the *AtMRP5* gene may have a defined function during silique ripening or abscision.

Table I. Characteristics of ATP-dependent β-oestradiol 17-(β-D-glucuronide) uptake into vesicles isolated from YYA4 yeasts transformed with pN-*At*MRP5

Condition	% of control
Control	100.0
1 mM vanadate	14.6 ± 6.4
0.1 μM bafilomycin A1	85.5 ± 1.6
5 mM NH_4Cl	90.0 ± 6.0
150 μM glibenclamide	10.6 ± 6.1
0.2 mM luteolin 7-*O*-diglucuronide (4′-*O*-glucuronide)	33.4 ± 7.5
0.2 mM oestradiol sulfate	0.2 ± 3.5
0.2 mM glycocholate	13.9 ± 6.4
3 mM GSH	80.7 ± 4.6
3 mM GSSG	71.6 ± 4.8
0.2 mM DNB-GS	74.4 ± 5.9

Yeast vesicles were incubated with 10 μM [^{3}H]$E_2$17G in the presence of 5 mM MgATP and the inhibitors and potential competitors indicated. After 8 min, uptake was terminated by transfer of three aliqouts onto Durapore filters. Values are corrected for corresponding controls with vesicles isolated from YYA4 yeasts transformed with the empty NEV vector. Due to the variability of the uptake activities in different preparations, uptake rates were standardized to 100%, which corresponds to 7–25 pmol $E_2$17G/mg protein/min. The different inhibitors and competitors were always tested using the same vesicle preparation.

Isolation and characterization of a T-DNA knockout mutant for AtMRP5

In plants, MRPs are considered to play a role in detoxification. However, the large number of these

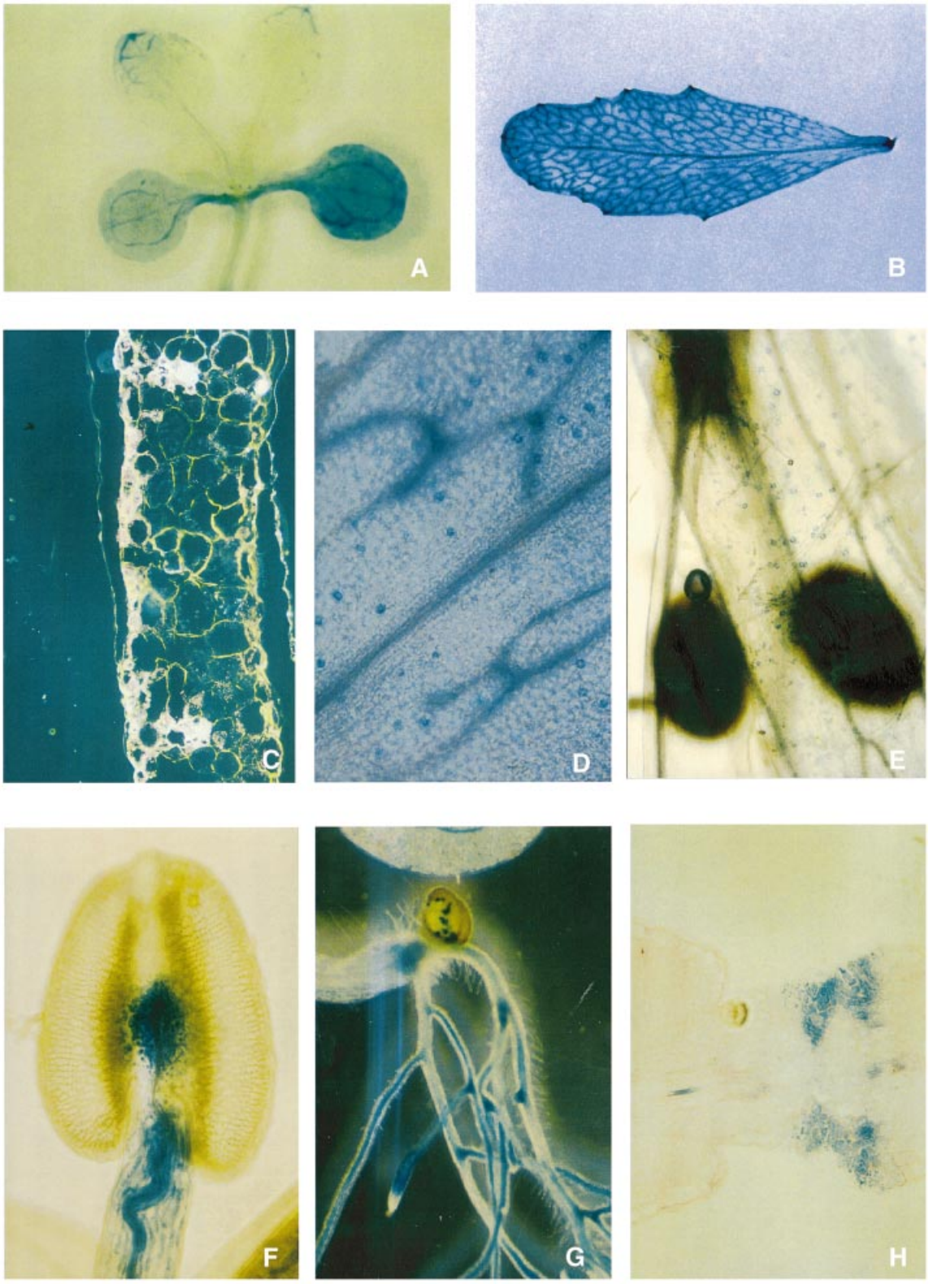

Fig. 3. Histochemical localization of GUS activity. (**A**) A seedling at 7 days after germination (dag) showing GUS expression in cotyledons and vascular tissue in the tip of primary leaves. (**B**) The leaf of an *Arabidopsis* plant 21 dag exhibiting GUS expression in lower and higher order veins. (**C**) Dark-field observation of a cross-section of an adult leaf with GUS expression in vascular tissue, epidermal cells and weakly in mesophyll cells. (**D**) The abaxial epidermis of an adult leaf exhibits strong GUS staining in guard cells. (**E**) Flower petals showing GUS expression in guard cells. (**F**) GUS staining in pollen sacs is present along the central vascular strand of the filament and in connecting tissue. (**G**) The root of a seedling at 11 dag. GUS expression is present in the central cylinder but not in root tips. (**H**) GUS staining at the pod attachment site.

Table II. Segregation of the kanamycin resistance marker of *mrp5-1* T-DNA mutant crosses into the Wassilewskia wild type (Ws-2)

Generation	No. of plants	Selection on kanamycin	
		No. Kan^R (%)	No. Kan^S (%)
P (*mrp5-1* parent)	109	109 (100)	0 (0)
F_2 *mrp5-1* × Ws-2	255	199 (78.0)	56 (22.0)
F_3 *mrp5-1* × Ws-2 of a *mrp5-1*/*mrp5-1* F_2 parent	278	278 (100)	0 (0)
F_3 *mrp5-1* × Ws-2 of a *mrp5-1*/Ws-2 F_2 parent	311	225 (72.4)	86 (27.6)
F_3 *mrp5-1* × Ws-2 of a Ws-2/Ws-2 F_2 parent	243	0 (0)	243 (100)

In the F_3 plants, seeds of single F_2 parents that were found to represent *mrp5-1*/*mrp5-1*, *mrp5-1*/Ws-2 and Ws-2/Ws-2 genotypes by Southern analysis (see Figure 3) were analysed.

transporters and specific expression patterns indicate that they have specific functions. The analysis of mutants is a valuable tool to help to discover the role of a particular gene in physiological and developmental functions in plants. Using this approach, the action of gene products in their cellular context can be studied.

We identified a T-DNA knockout mutant for *AtMRP5*, called mrp5-1, in a collection of 4120 T-DNA-transformed lines from seed transformation (Forsthoefel *et al*., 1992) using a reverse genetic PCR-based screening strategy. Sequence analysis of a PCR fragment amplified with the primer combination MRP35A-anti (sequence-specific)/RB2 (T-DNA primer) on genomic DNA of *mrp5-1* revealed a T-DNA inserted into *AtMRP5* at position +1420. For further characterization of the T-DNA insertion, two additional primers, flanking the site of the T-DNA insertion, were designed. One of these primers, MRP5D-sense, was used in combination with the T-DNA primers LB2 and RB2 to amplify the junction sequence of the T-DNA and the 3′ region of *AtMRP5* in *mrp5-1*. Sequencing of the resulting PCR fragment amplified with LB2 and MRP5D-sense showed the insertion of T-DNA with left border sequences facing the *MRP5* locus at position +1471. This analysis revealed that T-DNA integration into the first exon of *MRP5* occurred with intact left and right border sequences and resulted in a deletion of 52 bp at the integration site.

Two findings suggested that mrp5-1 isolated from the screen was homozygous for the T-DNA insertion. (i) All PCRs carried out on genomic DNA isolated from >20 individuals of the offspring of the isolated plant resulted in PCR products of the correct size with the combination of primers specific for *At*MRP5 and the T-DNA. In contrast, all PCRs performed with the MRP5D-sense/MRP5D-anti primer combination gave no fragment amplification. This indicated that all plants carried the T-DNA and none possessed the wild-type allele. (ii) More than 100 seeds of the primary mrp5-1 plant isolated were tested for segregation of the kanamycin resistance marker of the 3850:1003 T-DNA construct (Velten and Schell, 1985). All exhibited a resistant phenotype in the presence of this antibiotic, which is expected for a homozygous T-DNA transformant (Table II).

Feldmann (1991) concluded that the average number of independent T-DNA inserts in this collection is ~1.5 per diploid genome. In order to analyse the genotype of *mrp5-1* and to select homozygous mutant plants carrying a T-DNA insertion at a single insertion locus, the *mrp5-1* plant was crossed with the Wassilewskia (Ws-2) wild type. After self-pollination of the F_1 generation, genomic DNA of 90 resulting F_2 plants was subjected to restriction digestion and DNA gel blot analysis using probes for the *AtMRP5* gene and the T-DNA borders. In Figure 4, corresponding results are depicted for genomic DNA isolated from six single plants with different genotypes. A shift in size of hybridizing bands after hybridization with a gene-specific probe allowed the identification of plants that were homozygous for the T-DNA insertion. The expected size for hybridizing bands from insertion alleles could be calculated on the basis of the physical map of the *AtMRP5* locus in conjunction with the physical map of the integrated T-DNA (Figure 4A). Furthermore, hemizygous plants could be identified by the presence of hybridizing bands that showed the same shift in size as the bands in plants that were homozygous for the T-DNA insertion. In addition to these signals, the hybridization pattern of wild-type plants is also present in hemizygous plants (Figure 4B). Hybridization signals with a probe specific for T-DNA left border sequences were detected only in hemizygous plants and plants homozygous for the T-DNA insertion (Figure 4C). Single bands found exclusively in hemizygous and homozygous mutants were also detected when a right border T-DNA fragment was used as a probe (data not shown).

On selective medium, the F_2 generation of the *mrp5-1*/Ws-2 backcross segregated in a ratio of ~3:1 for the kanamycin marker (Table III). The F_3 generation of homozygous mutants selected through the results of the DNA blot analysis was 100% resistant, while hemizygous mutants again segregated in a 3:1 ratio. Thus, DNA blot analysis and the segregation of the kanamycin marker in the *mrp5-1*/Ws-2 backcross proved that mrp5-1 plants carry a single T-DNA insertion in the *AtMRP5* gene.

In order to investigate *AtMRP5* transcript levels, we performed RT–PCR on total RNA isolated from homozygous mrp5-1 knockout plants using the primer pair MRP5D-sense and MRP5D-anti, which would amplify the gene region where the T-DNA insertion is located. While RT–PCR with RNA isolated from wild-type Ws-2 plants clearly confirmed the presence of *AtMRP5* transcripts, no mRNA was detectable in knockout plants (Figure 4D).

mrp5-1 mutants exhibit a strongly reduced root growth

Since heterologously expressed *At*MRP5 mediated organic anion transport in yeast (Figure 3; Tables I and II), we were interested in whether the transtonoplast transport of a GS-X was reduced in adult mrp5-1 plants.

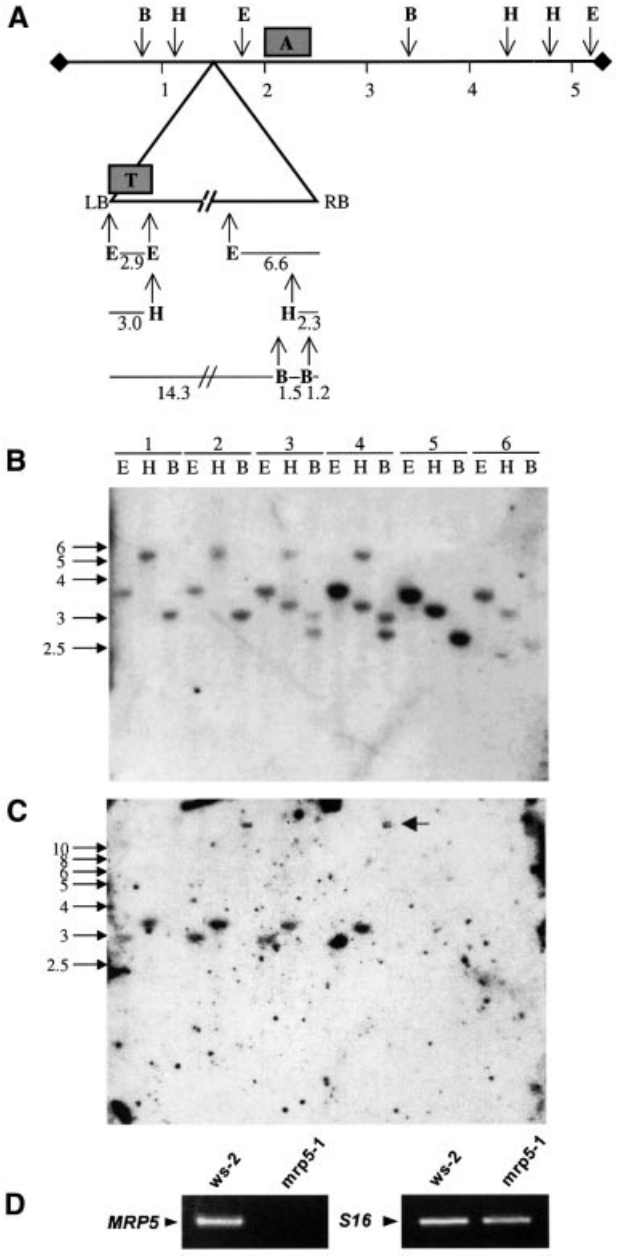

Fig. 4. DNA blot analysis of six singular F_2 plants of the *mrp5-1*/Ws-2 crossing exhibiting *mrp5-1*/*mrp5-1* (lanes 1 and 2 in B and C), *mrp5-1*/Ws-2 (lanes 3 and 4) and Ws-2/Ws-2 (lanes 5 and 6) genotypes (A–C) and RT–PCR analysis of *mrp5-1*/*mrp5-1* plants (D). (**A**) Schematic view of the 5.6 kb genomic sequence of *AtMRP5* and of the 17 kb T-DNA construct 3850:1003 (Schulz *et al*., 1995) inserted in *mrp5-1* (triangle) with predicted restriction sites of enzymes *Eco*RI (E), *Hin*dIII (H) and *Bam*HI (B) (numbers indicate relative positions in kb). The position of the gene-specific probe and a probe specific for the T-DNA left border are indicated as boxes denoted A and T, respectively. (**B**) DNA blot analysis of genomic DNA digested with *Eco*RI, *Hin*dIII and *Bam*HI probed with the gene-specific probe A. (**C**) The same as (B) using the T-DNA probe T. The arrow highlights the 15 kb band visible after restriction with *Bam*HI. (**D**) RT–PCR analysis of *AtMRP5* and *S16* expression in Ws-2/Ws-2 and *mrp5-1*/*mrp5-1* plants.

Monochlorobimane is readily converted in the cytosol to form the fluorescent bimane–GS conjugate followed by vacuolar transfer of the dye via MRP-like ABC transporters (Coleman *et al*., 1997). The incubation of leaf mesophyll protoplasts from Ws-2 and mrp5-1 plants showed no significant difference in the vacuolar fluorescence (data not shown). However, since the accumulation was variable between one cell and another in the wild type as well as in the mutants, the possibility cannot be excluded that uptake of GS-X was reduced in some cell types of the mutant normally exhibiting stronger expression of *AtMRP5*.

Seeds of homozygous mrp5-1 were surface sterilized and germinated on vertical plates with sterile 0.5× Murashige and Skoog (MS) medium supplemented with 1% sugar in a 16 h–8 h light–dark cycle or under continuous light. Up to 4 days after germination (dag), all seedlings showed typical wild-type morphology when compared with Ws-2 plants. Starting with day 5, the root elongation of mrp5-1 seedlings was strongly reduced and mutant plants initiated the lateral and secondary roots earlier than wild-type seedlings (Figure 5A–C). In all our experiments, hypocotyl length and leaf morphology were not visibly affected in mrp5-1 seedlings (data not shown).

The morphology of the entire root system of mrp5-1 seedlings grown vertically under continuous light for 24 days appeared to be more branched than that of Ws-2 seedlings (Figure 5E). In contrast, the development of root hairs in mrp5-1 was normal (Figure 5B). The aerial parts of adult mrp5-1 plants grown on soil in either a 10–14 h or 16–8 h light–dark cycle exhibited wild-type morphology at all stages of development (data not shown).

Under high nutrient culture conditions (1× MS medium), the effect on root growth appeared reversed: mrp5-1 plants produced short but visible roots, while root growth of Ws-2 was extremely reduced (Figure 5F).

In order to investigate the phenotype of mrp5-1 plants on 0.5× MS medium in more detail, we continuously recorded the development of Ws-2 and mrp5-1 plants using a time-lapse video system (Table III). In a first experiment, simple vertical growth of mrp5-1 and Ws-2 seedlings was recorded for 300 h. During germination, onset of primary roots as well as cotyledons and primary leaves differed insignificantly. Later, the root growth rate of mrp5-1 was only half of that observed for Ws-2 seedlings. In comparison with Ws-2, lateral and secondary roots initiated ~50 h earlier in mrp5-1 seedlings. At 220 h after germination, only 40% of Ws-2 seedlings developed a lateral root, while 90% of mrp5-1 seedlings showed formation of one or more lateral roots. In most seed batches, root growth was inhibited ~50%; however, it must be mentioned that in a minority of seed batches root growth was reduced only 20–30%.

In a second experiment, the gravitropic reaction of mrp5-1 roots was analysed. Seedlings grown for 6 days were turned at a 90° angle and the direction of root growth was recorded. No difference in the gravitropic response was observed between wild type and mutant.

Increased auxin levels in roots of mrp5-1 plants

The phenotype observed for mrp5-1 plants grown in standard 0.5× MS/1% sucrose medium suggested that under these conditions increased auxin levels could inhibit primary root growth but induce lateral root development. Indeed, auxin levels were increased by a factor of ~2 in roots of mutant plants (Table IV). Since auxin levels of plants grown on different plates differed, probably due to slight differnces in light intensity, we always calculated

Table III. Characteristic features of germination and development of wild-type (Ws-2) and *mrp5-1* mutant seedlings

Feature		Ws-2	*mrp5-1*
Appearance of primary root/germination	first seedling	29 h	30 h
	10 seedlings	35 h	33 h
	all seedlings	41 h	45 h
Primary root length 2 mm	first seedling	45 h	39 h
	10 seedlings	49 h	52 h
	all seedlings	56 h	59 h
Root growth velocity after arriving at 2 mm length		5 h 40 min per mm	12 h 16 min per mm
First lateral roots appearing		191 h	136 h
First secondary roots appearing		192 h	141 h
No. of plants with lateral roots after 220 h growth	no lateral roots	12	2
	1 lateral root	5	9
	>2 lateral roots	3	9
No.of plants with secondary roots after 220 h growth		4	18
Appearance of cotyledons	10 seedlings	60 h	62 h
Primary leaves visible	10 seedlings	187 h	180 h
Dimensions of grains in μm		452 ± 39 × 267 ± 19	473 ± 35 × 265 ± 33

The growth of 20 plants was analysed using a time-lapse video system: 1 min on the video corresponded to 80 min real time. Sterile seeds were grown on 1/2× MS with 1% sucrose and 0.8% agar after 48 h vernalization at 4°C in the laboratory with constant light coming from the side (neon light). Typical features of a vertical growth test are reported. Plant growth was recorded over a total time of 300 h. The average dimensions of mutant and wild-type grains are given: 20 grains were measured using a scanning electron microscope.

the ratio of auxin in mutant and wild-type plants grown on the same plate.

AtMRP5 controls glibenclamide-dependent stomata opening

The high similarity of *At*MRP5 to CFTR and SUR, together with the facts that *At*MRP5 was strongly expressed in guard cells and that its transport activity was inhibited by glibenclamide, prompted us to investigate whether *At*MRP5 might control ion fluxes in guard cells. Stomatal movement is mediated by anion and K^+ fluxes from guard cells and it has been shown previously that glibenclamide, a well known modulator of K-ATP channels and CFTR chloride channels (Schmid-Antomarchi *et al*., 1987; Sheppard and Welsh, 1992), is involved in the regulation of ionic channels in guard cells (Leonhardt *et al*., 1997, 1999). As already demonstrated in other species, glibenclamide triggered stomatal opening in darkness in *Arabidopsis* wild-type plants in a dose-dependent manner. In contrast, stomatal opening induced by glibenclamide was completely abolished in mrp5-1 plants (Figure 6).

Discussion

Data from the sequencing project of the *Arabidopsis* Genome Initiative revealed the presence of a large number of genes exhibiting sequence similarities to ABC transporters. For most of their gene products, a physiological role is still unknown. The best characterized plant ABC transporter is the MRP subfamily. For three of its members, *At*MRP1, *At*MRP2 and *At*MRP3, preliminary functional data are available (Lu *et al*., 1997, 1998; Tommasini *et al*., 1998; Liu *et al*., 2001). All of them exhibit directly energized uptake of organic anions such as GS-Xs. Similar transport activities have been demonstrated for isolated vacuoles or vacuolar membrane preparations (Rea *et al*., 1998; Martinoia *et al*., 2000). A database search for homologues of *At*MRPs revealed 14 members of this subfamily in *Arabidopsis*. In analogy to the transport functions for known MRPs in animals, yeast and plants, it can be assumed that most of them exhibit partially overlapping, ATP-dependent transport activities for organic anions. In order to address the specific role of *At*MRP5, a novel member of this gene family, during plant development, we performed a detailed analysis integrating biochemical and genetic strategies.

Organic anions are recognized by AtMRP5

Heterologous expression of *At*MRP5 in the GS-X transport-deficient yeast mutant Δ*ycf1* (Szczypka *et al*., 1994) indicated that *At*MRP5 is a low capacity ATP-dependent GS-X transporter. Since similar activities were reported for the majority of characterized MRPs in animals, yeast and plants, it could be argued that GS-X transport is a common and evolutionarily conserved feature of MRPs. It is tempting to speculate that in the few cases where such an activity has not been reported, the respective MRP nevertheless is able to transport GS-Xs, but that this activity is low compared with the transport activity for other solutes. In addition to GS-Xs, *At*MRP5 was also able to transport the model glucuronide $E_2$17G, a substance produced during the catabolism of steroids in animals but not known in plants. Transport studies with isolated plant vacuoles demonstrated the existence of a ubiquitous vacuolar ABC-type transport system for different

Fig. 5. The *mrp5-1* mutant displays a reduction in root growth. (**A**) Light-grown *mrp5-1* (upper row) and Ws-2 (lower row) seedlings 8 days after germination (dag) grown vertically on 1/2× MS/1% sucrose plates. (**B**) A single *mrp5-1* plant at higher magnification exhibiting lateral roots. (**C**) Comparison of Ws-2 (closed circles) and mrp5-1 (open circles) primary root length. Each data point represents the average of 20 seedlings. (**D**) Reaction of seedling growth after change of the gravitropic angle. Three *mrp5-1* (upper row) and three Ws-2 (lower row) seedlings 11 dag grown on vertical plates. Plates were turned 4 dag. (**E**) Twenty six-day-old plants grown on vertical plates in the light. The three mrp5-1 seedlings on the left exhibit bushy roots due to the presence of more root branches when compared with the three Ws-2 plants on the right. (**F**) Seedlings 10 dag grown on a medium corresponding to 1× MS (for details see Supplementary data). (A, B and D) Length of squares = 2 cm; (E and F) bar = 1 cm.

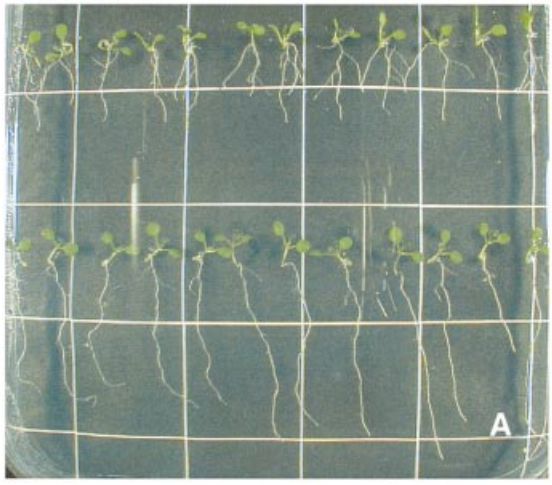
A

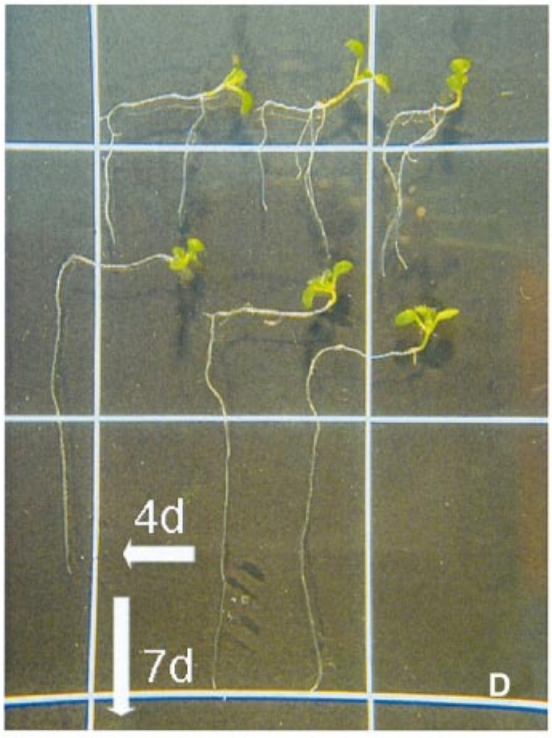
4d
7d
D

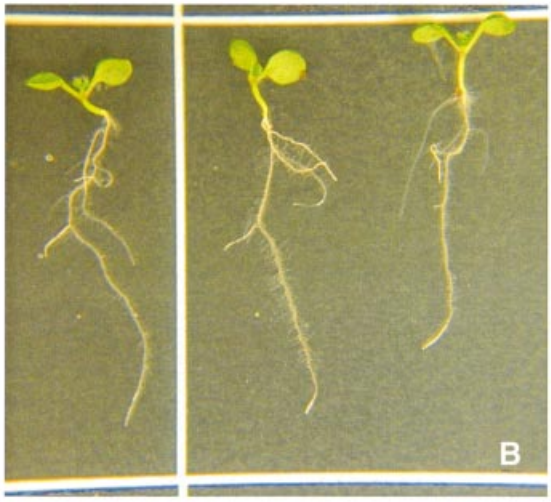
B


E

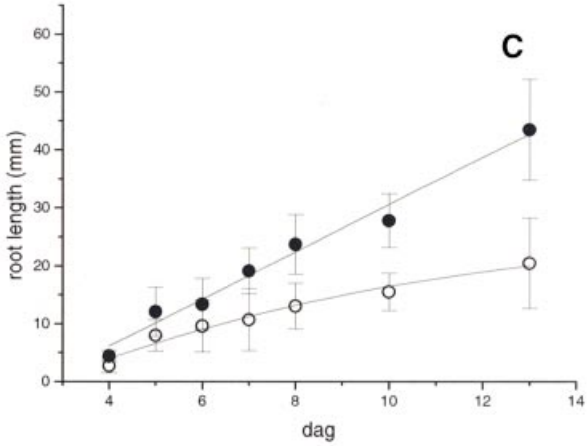
C
root length (mm)
dag
0
10
20
30
40
50
60
4
6
8
10
12
14

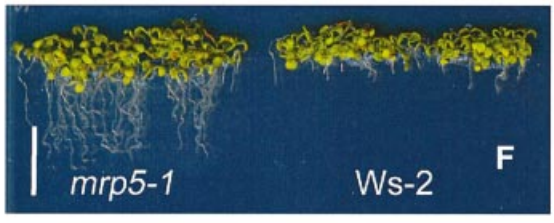
mrp5-1
Ws-2
F

Table IV. The level of free auxin is increased in roots of the *mrp5-1* T-DNA mutant

	Ratio of IAA/mg fresh weight in *mrp5-1* versus Ws-2 roots (*n*)
Experiment 1	2.11 ± 0.63 (3)
Experiment 2	1.57 ± 0.31 (3)
Experiment 3	2.02 ± 0.12 (4)

For the analysis of free auxin, 40–80 whole roots of *mrp5-1* or Ws-2 plants grown vertically for 10 days were cut, removed, and after determination of the fresh weight, extracted with MeOH in the presence of [$^2H_2$]IAA as a standard. Auxin was measured by GC–MS. Each experiment consisted of three or four independent determinations analysing various seed batches and different positions of the seedlings on the plate. Due to variations between different plates, the ratios were determined from *mrp5-1* and Ws-2 samples grown on the same plate. The absolute IAA content of all independent determinations in Ws-2 roots ranged between 107 and 279 fmol/mg of fresh weight.

glucuronides (Klein *et al*., 1998, 2000). Glutathione and its conjugates were found to act as modulators of the vacuolar glucuronide uptake activity. The vacuolar transport rate for $E_2$17G and flavone glucuronides was strongly increased in the presence of the conjugate DNB-GS. A comparable complex stimulation was observed for *At*MRP2 expressed in Δ*ycf1* (Liu *et al*., 2001). In contrast, we could not observe such a modulation for *At*MRP5, indicating either that *At*MRP5 does not represent a glucuronide transporter of the central vacuole or that *At*MRP5 is not or is only weakly expressed in mesophyll cells and exhibits properties other than as the main glucuronide transporter of mesophyll vacuoles. To our knowledge in human and animal MRPs, glucuronide transport activity is not strongly increased in the presence of certain GS-Xs and, therefore, the transport properties of *At*MRP5 approximate more those of the animal MRPs.

Expression analysis suggests a role for AtMRP5 in vascular tissues and in the epidermis

In order to learn more about the function of *At*MRP5, we investigated its expression by northern analysis, RT–PCR and with transgenic plants expressing a promotor–GUS fusion construct. Northern analysis as well as RT–PCR indicated that *AtMRP5* is expressed in all parts of the plant. A similar picture was observed for *AtMRP1*, *AtMRP2* and *AtMRP3* (Tommasini *et al*., 1997). Promotor–GUS fusions allowed us to investigate the expression pattern of *At*MRP5 in more detail. Strong GUS expression was found in the vascular tissue of all organs and in the epidermis including stomata, while the expression level in mesophyll cells was low. Expression of *At*MRP5 in guard cells is consistent with the fact that multiple *cis*-acting T/AAAAG elements are located in the *AtMRP5* promoter close to the transcriptional start site (not shown), which are major determinants of guard cell gene expression (G.Plesch, T.Ehrhardt and B.Mueller-Roeber, unpublished data).

AtMRP5 affects root growth

Using a reverse genetic approach, we demonstrated for the first time that plant MRPs can play an important role in organ development. Recently, Sidler *et al*. (1998) reported that modulation of the expression of the MDR homologue

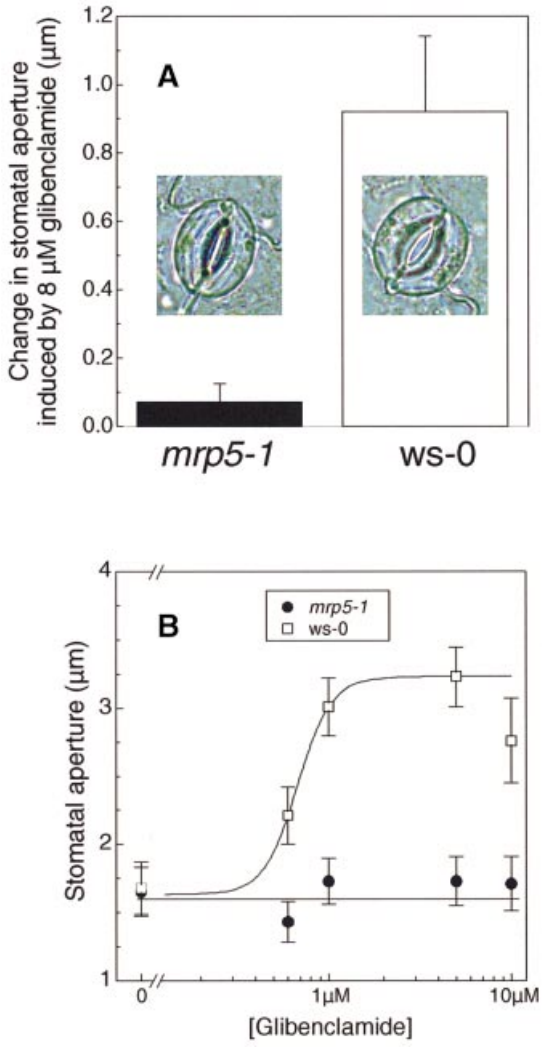

Fig. 6. Stomata of mrp5-1 plants are insensitive towards the sulfonylurea glibenclamide. (**A**) The change in stomatal aperture was measured as the difference between aperture values in the presence and absence of 8 µM glibenclamide. Each column represents the mean of five independent experiments (±SEM) each conducted on five plants. The aperture of 60 stomata was determined per experiment. Individual stomata exposed for 3 h are illustrated in the respective columns. (**B**) A representative experiment showing that application of glibenclamide for 3 h in the dark produces a dose-dependent increase in stomatal aperture in the wild-type plant (open squares) but not in the *mrp5-1* plants (solid circles). Half-maximal opening of stomata is at 0.8 µM glibenclamide.

AtPGP1 in antisense and overexpressing plants resulted in altered hypocotyl elongation. Under certain light fluence rates, hypocotyl elongation was increased in *At*PGP1-overexpressing plants and decreased in antisense plants. However, the transport function of *At*PGP1, a plasma membrane protein, is still a matter of debate.

Homozygous *mrp5-1* mutant plants showed a strongly reduced root elongation associated with an earlier initiation of lateral root formation (Table IV; Figure 5). The analysis of growth kinetics under continuous light revealed that following the very early stages of germination (up to 4 dag) where no visible differences could be observed, the velocity of root growth was reduced to ~50% compared with wild-type root development. The observation that in gravitropic response experiments root growth remained decreased after turning the plates (Figure 5) and the fact

that grains measured by scanning microscopy did not exhibit size differences between mrp5-1 and Ws-2 grains (Table III) suggests that reduced root growth is not due to decreased nutrient availability in the grains of mutant plants.

It is well known that elevated levels of free auxin inhibit root growth and induce formation of lateral roots. Indeed, we found increased levels of auxin in roots of the ABC transporter mutant (Table IV). Auxin is synthesized in apical growing regions of the plant, especially in developing primary leaves. From these tissues, it is transported unidirectionally to the root of a plant through the vascular system. Two transport systems are known (Palme and Gälweiler, 1999). *AUX1* is responsible for auxin uptake into the cell (Bennett *et al*., 1996; Marchant *et al*., 1999), while members of the *PIN* gene family catalyse its efflux (Gälweiler *et al*., 1998; Müller *et al*., 1998). The root phenotype observed for mrp5-1 could be explained either by a direct interaction of *At*MRP5 with auxin homeostasis or by secondary effects such as changes in ion conductance that consequently alter phytohormone levels. In the first case, *At*MRP5 could act as a transporter for auxin conjugates such as the negatively charged indole acetic acid (IAA)-aspartate or IAA-glutamate (Östin *et al*., 1998; Tam *et al*., 2000). It has been shown that *Hs*MRP1 is able to transport glutamate conjugates (König *et al*., 1999). According to this hypothesis, the phenotype of mrp5-1 could be explained by a model where, in the absence of *At*MRP5, inefficient removal of auxin conjugates formed in the cytosol results in a slight increase in free auxin. Alternatively, *At*MRP5 may interact with channels and modulate their activities in the roots as observed in the stomata (see below), resulting in a decreased potassium or anion uptake. Under nutrient stress, plants could form more lateral roots, a process that may be triggered by increased auxin concentrations. Presently, the possibility cannot be excluded that both processes, reduced auxin conjugate transport and nutrient uptake, occur simultaneously.

AtMRP5 is implicated in stomata regulation

Pharmacological studies of ion fluxes using glibenclamide and other drugs in guard cells suggest the presence of SUR- and/or CFTR-like ABC proteins controlling stomatal aperture (Leonhardt *et al*., 1997, 1999). We observed that glucuronide transport activity of *At*MRP5 could be inhibited by the sulfonylurea glibenclamide (Table I) and that *At*MRP5 is expressed mainly in the vascular tissue and the epidermis, including the guard cells (Figure 6). Therefore, we investigated whether stomata of mrp5-1 plants were affected in their response to glibenclamide. The insensitivity of stomata from mutant plants to glibenclamide suggests that *At*MRP5 controls either K^+ or anion channels. However, the possibility cannot be excluded that *At*MRP5 itself acts as a channel or is a member of the signal transduction pathway leading to stomata opening. Future studies will show at which level *At*MRP5 is involved in stomata regulation.

Materials and methods

Plant material and growth conditions

If not stated otherwise, plants were grown on soil under a 16 h light–8 h dark regime. For epidermal strip experiments, plants were grown individually in pots of sand watered with half-strength Hoagland's solution in a growth chamber with 8 h light–16 h dark. For the analysis of the phenotype of mrp5-1, surface-sterilized and vernalized seeds (48 h at 4°C) were germinated on half-strength MS salts (Duchefa, M0233, NL) with 1% sucrose under continuous light. For the medium used in Figure 5F, see the Supplementary data, available at *The EMBO Journal* Online.

Cloning of AtMRP5 cDNA

A nested PCR was performed on an EST (DDBJ/EMBL/GenBank accession No. W43620) encoding a putative ABC transporter from *Arabidopsis*. The resulting 244 bp DNA fragment was used to isolate a full-size cDNA of 5.1 kb by screening 1×10^6 plaque-forming units of a hypocotyl cDNA library. The transcriptional start site of the *AtMRP5* gene was determined by RACE-PCR. Sequence similarities were identified by using default parameters of the BESTFIT program. The *AtMRP5* cDNA sequence has been deposited in the DDBJ/EMBL/GenBank database (accession No. Y11250).

Northern and Southern blot analysis

For northern blots, RNA was isolated from different tissues of *A.thaliana* as described by Chomczynski and Sacchi (1987). Northern (40 µg of total RNA) and Southern (10 µg of DNA) blots were performed following standard protocols (Sambrook *et al*., 1989). Northern blots were hybridized with a 0.7 kb *Eco*RI–*Nhe*I fragment of the 5′ region of the *AtMRP5* cDNA. DNA gel blots performed to analyse the PCRs in reverse genetic screens and to investigate the genotype of *mrp5-1* mutant plants were hybridized with a probe generated by PCR using Ws-2 genomic DNA and primers MRP5An-sense and -anti (see Table V). T-DNA-specific probes were a 6.5 and a 3.5 kb *Hin*dIII fragment containing the left and right border of 3850:1003, respectively (Jones *et al*., 1987). For RT–PCR analysis of Ws-2 and *mrp5-1*, total RNA from seedlings grown in liquid cultures under mixotrophic conditions (1× MS, 1% sucrose; constant light) for 7 days was prepared using the RNeasy Plant Kit (Qiagen). Oligo(dT)-primed cDNA from 1 µg of total RNA was synthesized using the Reverse Transcription system (Promega). MRP5- and 40S ribosomal protein S16-specific cDNAs were amplified by PCR for 30 or 25 cycles, respectively, at 52°C. RT–PCR primers used were: S16-upper 5′-ggcgactcaaccagctactga and S16-lower 5′-cggtaa-ctcttctggtaacga for S16, and MRP5D-sense and -anti (Table V) for *AtMRP5*.

Isolation of the AtMRP5 promoter and GUS expression analysis

The structural organization of the *AtMRP5* gene was deduced from genomic Southern blots (not shown) and the sequence of BAC clone F20D22 (DDBJ/EMBL/GenBank accession No. AC002411). Partial digestion of *Arabidopsis* genomic DNA with *Hin*dIII–*Bgl*II and *Xba*I–*Bgl*II yielded fragments of 3 and 1.8 kb, which were fused to produce promoter–GUS constructs. *Arabidopsis thaliana* (col-0) plants were transformed using *Agrobacterium* and vacuum infiltration (Bechthold *et al*., 1993). Selected transformants were assayed for GUS activity (5 h incubation at 37°C, unless stated otherwise) using X-Gluc (Duchefa) as substrate. For microscopic analysis, GUS-stained plant tissue was embedded in Technovit 7100 (Kulzer, Wertheim, Germany) and 8 µm sections were cut with a microtome (RM2155, Leica, Germany). Specimens were stained with 5% fuchsin (Sigma) for 20 min before microscopy (Olympus AX-70 microscope).

Table V. Primers used for the identification and verification of the *mrp5-1* mutant, for the generation of probes and RT–PCR analysis

Primer name	Primer sequence
RB2	5′-TCCTTCAATCGTTGCGGTTCTGTCAGTTC-3′
LB2	5′-GATGCACTCGAAATCAGCCAATTTTAGAC-3′
MRP35A-sense	5′-TGTGGYACMGTTGGCTCTGGRAAATC-3′
MRP35A-anti	5′-GTGTGTGCATCMASAGCRCTAAAAGG-3′
MRP5An-sense	5′-CTTGCATCCTAGGGGAAATCCCAAAAA-3′
MRP5An-anti	5′-TAATGCCCTTGCAAGTTGTACACGC-3′
MRP5D-sense	5′-GCGCATAGGAGATTACTCATGGTATC-3′
MRP5D-anti	5′-CCGAAGTGGCTCCTGAAGAATACAGA-3′

LB2 and RB2 represent primers specific for the T-DNA left and right border, respectively.

Expression of AtMRP5 in yeast, preparation of yeast microsomes, uptake experiments and analysis of cadmium sensitivity

The *AtMRP5* cDNA was cloned into pNEV (Tommasini *et al*., 1996) to give pN-*At*MRP5. pNEV and pN-*At*MRP5 were introduced into yeast strains DTY168 (Szczypka *et al*., 1994) and YYA4 (*Mata, Δycf1::loxP-KAN-loxP, Δyhl035::HIS3, ade2-1, his3-11,-15, leu2-3, 112 trp1-1, ura3-1, can1-100*). Microsomes for transport analysis were isolated as described (Tommasini *et al*., 1996). Uptake of 40 μM [^{14}C]DNB-GS or 10 μM [^{3}H]$E_2$17G was measured by rapid filtration using nitrocellulose (0.45 μm pore size) or Durapore® filters (0.22 μm pore size; Millipore GmbH, Eschborn, Germany), respectively. Analysis of Cd^{2+} tolerance of yeast strains DTY168, DTY7, DTY168-pN-*At*MRP5 or DTY168-pNev was performed as described (Tommasini *et al*., 1996).

Isolation of mrp5-1

The pooling strategy for plants and DNAs of T-DNA lines as well as DNA isolation for the reverse genetic screen will be described elsewhere (U.Kolukisaoglu, A.Möller and B.Schulz, in preparation). In this study, a collection of 4120 T-DNA transformed lines from seed transformation (Forsthoefel *et al*., 1992) arranged in pool sizes of 20, 100 and 500 independent lines was screened. An individual T-DNA insertion mutant named *mrp5-1* was identified by PCR and confirmed by subsequent sequencing of the PCR product. To analyse both gene regions flanking the T-DNA integration site in *AtMRP5*, PCRs were performed on genomic DNA of the isolated mutant plant using one of the *At*MRP5D primers in combination with border primers. PCR products were again subcloned and sequenced. For primer sequences, see Table V.

Extraction of plant material and auxin measurement

Roots (8–10 dag; 20–80 mg fresh weight) were immersed in 1 ml of methanol with 30 pmol of [$^{2}H_2$]IAA and incubated for 60 min at 37°C and 1–2 h at room temperature. The methanolic extract was concentrated to dryness in a stream of nitrogen. The residue was redissolved in 100 μl of diethylether and applied to 30 μl bed volume Bondesil NH_2 (Varian, Darmstadt). After washing with chloroform:isopropanol (2:1, 100 μl), the compounds were eluted with 200 μl of acidic diethylether (2% formic acid). This fraction was again dried, redissolved in 50% aqueous methanol and then applied to 10 μl bed volume ENV+ (IST, Mid Glamorgan, UK). The liquid was removed from the solid phase by a stream of nitrogen. Compounds were eluted with 100 μl of etheral diazomethane, dried and dissolved in 5 μl of chloroform. An aliquot of 1 μl was subjected to gas chromatography–mass spectroscopy (GC–MS) using a Varian Saturn 2000 ion trap mass spectrometer.

Growth analysis and epidermal strip experiments

Primary root length was measured with seedlings grown on vertical plates every 24 h starting at 4 dag. Leaves from 4- to 5-week-old plants were harvested in the dark at the end of the night period and placed with their abaxial side onto a transparent medical adhesive-coated coverslip. The adaxial epidermis and mesophyll were removed using a razor blade. The coverslip was then placed in a Petri dish containing 10 mM KCl, 30 mM KOH, 25 mM iminodiacetate and 10 mM MES pH 6.5 at 20°C. After 30 min in the dark, glibenclamide prepared as described (Leonhardt *et al*., 1997) was added to the solution and measurements of stomatal apertures for Ws-2 and *mrp5-1* mutant plants were performed after 3 h in the dark. Only 'mature stomata' whose ostiole length was greater than one-third the length of stoma were analysed. For each treatment, at least 60 stomatal apertures were measured. All experiments were repeated five times.

Supplementary data

Supplementary data for this paper are available at *The EMBO Journal* Online.

Acknowledgements

The authors wish to thank Aurélie Pedezert for excellent technical assistance, Dr M.Geisler for performing RT–PCR, and Laetitia Perfus-Barbeoch for help with stomatal bioassays. This work was supported by the Schweizerischer Nationalfonds (E.M.), the Humboldt Stiftung (M.K.), the Deutsche Forschungsgemeinschaft (B.M.-R. and B.S.) and the Commissariat à l'Energie Atomique (C.F.).

References

Anderson,M.P.,Gregory,R.J., Thompson,S., Souza,D.W., Paul,S., Mulligan,R.C., Smith,A.E. and Welsh,M.J. (1991) Demonstration that CFTR is a chloride channel by alteration of its anion selectivity. *Science*, **253**, 202–205.

Azpiroz-Leehan,R. and Feldmann,K.A. (1997) T-DNA insertion mutagenesis in *Arabidopsis*: going back and forth. *Trends Genet.*, **13**, 152–156.

Bechthold,N., Ellis,J. and Pelletier,G. (1993) *In planta Agrobacterium* mediated gene transfer by infiltration of adult *Arabidopsis thaliana* plants. *Mol. Biol. Genet.*, **316**, 1194–1199.

Bennett,M.J., Marchant,A., Green,H.G., May,S.T., Ward,S.P., Millner,P.A., Walker,A.R., Schulz,B. and Feldmann,K. (1996) *Arabidopsis AUX1* gene: a permease-like regulator of root gravitropism. *Science*, **273**, 948–950.

Bryan,J. and Aguilar-Bryan,L. (1999) Sulfonylurea receptors: ABC transporters that regulate ATP-sensitive K^+ channels. *Biochim. Biophys. Acta*, **1461**, 285–303.

Chomczynski,P. and Sacchi,N. (1987) Single-step method of RNA isolation by acid guanidinium thiocyanate–phenol–chloroform extraction. *Anal. Biochem.*, **162**, 156–159.

Cole,S.P.C. *et al*. (1992) Overexpression of a transporter gene in a multidrug-resistant human lung cancer cell line. *Science*, **258**, 1650–1654.

Coleman,J.O.D., Randall,R. and Blake-Kalff,M.M.A. (1997) Detoxification of xenobiotics in plant cells by glutathione conjugation and vacuolar compartmentalization a fluorescent assay using monochlorobimane. *Plant Cell Environ.*, **20**, 449–460.

Dudler,R. and Hertig,C. (1992) Structure of an *mdr*-like gene from *Arabidopsis thaliana. J. Biol. Chem.*, **267**, 5882–5888.

Feldmann,K.A. (1991) T-DNA insertion mutagenesis in *Arabidopsis*—mutational spectrum. *Plant J.*, **1**, 71–82.

Forsthoefel,N.R., Wu,Y., Schulz,B., Bennett,M.J. and Feldmann,K.A. (1992) T-DNA insertion mutagenesis in *Arabidopsis*: prospects and perspectives. *Aust. J. Plant Physiol.*, **19**, 353–366.

Gälweiler,L., Guan,C., Müller,A., Wisman,E., Mendgen,K., Yephremov,A. and Palme,K. (1998) Regulation of polar auxin transport by *At*PIN1 in *Arabidopsis* vascular tissue. *Science*, **282**, 2226–2230.

Gottesman,M.M. and Pastan,I. (1993) Biochemistry of multidrug resistance mediated by the multidrug transporter. *Annu. Rev. Biochem.*, **62**, 385–427.

Henikoff,S., Greene,E.A., Pietrokovski,S., Bork,P., Attwood,T.E. and Hood,L. (1997) Gene families: the taxonomy of protein paralogs and chimeras. *Science*, **278**, 609–614.

Higgins,C.F. (1992) ABC transporter: from microorganisms to man. *Annu. Rev. Cell Biol.*, **8**, 67–113.

Higgins,C.F. (1995) The ABC of channel regulation. *Cell*, **82**, 693–696.

Hinder,B., Schellenberg,M., Rodoni,S., Ginsburg,S., Vogt,E., Martinoia,E., Matile,P. and Hörtensteiner,S. (1996) How plants dispose of chlorophyll catabolites: directly energized uptake of tetrapyrrolic breakdown products into isolated vacuoles. *J. Biol. Chem.*, **271**, 27233–27236.

Hofmann,K. and Stoffel,W. (1993) TMbase—A database of membrane spanning protein segments. *Biol. Chem. Hoppe-Seyler*, **347**, 166.

Jones,J.D.G., Gilbert,D.E., Grady,K.L. and Jorgensen,R.A. (1987) T-DNA structure and gene expression in petunia plants transformed by *Agrobacterium tumefaciens* C58 derivatives. *Mol. Gen. Genet.*, **207**, 478–485.

Klein,M., Martinoia,E. and Weissenböck,G. (1998) Directly energized uptake of β-estradiol-17-(β-D-glucuronide) in plant vacuoles is strongly stimulated by glutathione conjugates. *J. Biol. Chem.*, **273**, 262–270.

Klein,M., Martinoia,E., Hoffmann-Thoma,G. and Weissenböck,G. (2000) A membrane-potential dependent, ABC-like transporter mediates the vacuolar uptake of rye flavone glucuronides. *Plant J.*, **21**, 289–304.

König,J., Nies,A.T., Cui,Y., Leier,I. and Keppler,D. (1999) Conjugate export pumps of the multidrug resistance protein (MRP) family: localization, substrate specificity and MRP2-mediated drug resistance. *Biochim. Biophys. Acta*, **1461**, 377–394.

Leier,I., Jedlitschky,G., Buchholz,U., Cole,S.P.C., Deeley,R.G. and Keppler,D. (1994) The MRP gene encodes an ATP-dependent export pump for leukotriene C4 and structurally related conjugates. *J. Biol. Chem.*, **269**, 27807–27810.

Leonhardt,N., Marin,E., Vavasseur,A. and Forestier,C. (1997) Evidence for the existence of a sulfonylurea-receptor-like protein in plants: modulation of stomatal movements and guard cell potassium channels by sulfonylureas and potassium channel openers. *Proc. Natl Acad. Sci. USA*, **94**, 14156–14161.

Leonhardt,N., Vavasseur,A. and Forestier,C. (1999) ATP binding cassette modulators control abscisic acid-regulated slow anion channels in guard cells. *Plant Cell*, **11**, 1141–1152.

Li,Z.-S., Szczypka,M., Lu,Y.-P., Thiele,D.J. and Rea,P.A. (1996) The yeast cadmium factor protein (YCF1) is a vacuolar glutathione *S*-conjugate pump. *J. Biol. Chem.*, **271**, 6509–6517.

Liu,G., Sanchez-Fernandez,R., Li,Z.-S. and Rea,P.A. (2001) Enhanced multispecifity of *Arabidopsis* vacuolar MRP-type ABC transporter, AtMRP2. *J. Biol. Chem.*, in press.

Lu,Y.-P., Li,Z.-S. and Rea,P.A. (1997) *AtMRP1* gene of *Arabidopsis* encodes a glutathione *S*-conjugate pump: isolation and functional definition of a plant ATP-binding cassette transporter gene. *Proc. Natl Acad. Sci. USA*, **94**, 8243–8248.

Lu,Y.-P., Li,Z.-S., Drozdowicz,Y.M., Hoertensteiner,S., Martinoia,E. and Rea,P.A. (1998) *At*MRP2, an *Arabidopsis* ATP binding cassette transporter able to transport glutathione *S*-conjugates and chlorophyll catabolites: functional comparison with *At*MRP1. *Plant Cell*, **10**, 267–282.

Marchant,A., Kargul,J., May,S.T., Muller,P., Delbarre,A., Perrot-Rechenmann,C. and Bennett,M.J. (1999) AUX1 regulates root gravitropism in *Arabidopsis* by facilitating uptake within root apical tissues. *EMBO J.*, **18**, 2066–2073.

Martinoia,E., Grill,E., Tommasini,R., Kreuz,K. and Amrhein,N. (1993) ATP-dependent glutathione *S*-conjugate 'export' pump in the vacuolar membrane of plants. *Nature*, **364**, 247–249.

Martinoia,E., Klein,M., Geisler,M., Sánchez-Fernández,R. and Rea,P.A. (2000) Vacuolar transport of secondary metabolites and xenobiotics. In Robinson,D.G. and Rogers,J.C. (eds), *Vacuolar Compartments. Annual Plant Reviews*. Vol. 5. Sheffield Academic Press, Sheffield, UK, pp. 221–253.

Müller,A. *et al*. (1998) *AtPIN2* defines a locus of *Arabidopsis* for root gravitropism control. *EMBO J.*, **17**, 6903–6911.

Müller,M., Meijer,C., Zaman,G.J.R., Borst,P., Scheper,R.J., Mulder,N.H., DeVries,E.G.E. and Jansen,P.L.M. (1994) Overexpression of the gene encoding the multidrug resistance-associated protein results in increased ATP-dependent glutathione *S*-conjugate transport. *Proc. Natl Acad. Sci. USA*, **91**, 13033–13037.

Östin,A., Kowalyczk,M., Bhalerao,R. and Sandberg,G. (1998) Metabolism of indole-3-acetic acid in *Arabidopsis*. *Plant Physiol.*, **118**, 285–296.

Palme,K. and Gälweiler,L. (1999) PIN-pointing the molecular basis of auxin transport. *Curr. Opin. Plant Biol.*, **2**, 375–381.

Rea,P.A., Li,Z.-S., Lu,Y.-P., Drozdowicz,Y.M. and Martinoia,E. (1998) From vacuolar GS-X pumps to multispecific ABC transporters. *Annu. Rev. Physiol. Plant Mol. Biol.*, **49**, 727–760.

Sambrook,J., Fritsch,E.F. and Maniatis,T. (1989) *Molecular Cloning: A Laboratory Manual*, 2nd edn. Cold Spring Harbor Laboratory Press, Cold Spring Harbor, NY.

Schmid-Antomarchi,H., De Weille,J., Fosset,M. and Lazdunski,M. (1987) The antidiabetic sulfonylurea glibenclamide is a potent blocker of the ATP-modulated K^+ channel in insulin secreting cells. *Biochem. Biophys. Res. Commun.*, **146**, 21–25.

Schulz,B., Bennett,M.J., Dilkes,B.D. and Feldman,K.A. (1995) T-DNA tagging in *Arabidopsis thaliana*: cloning by gene disruption. *Plant Mol. Biol. Manual*, **K3**, 1–7.

Sheppard,D.N. and Welsh,M.J. (1992) Effect of ATP-sensitive K^+ channel regulators on cystic fibrosis transmembrane conductance regulator chloride currents. *J. Gen. Physiol.*, **100**, 573–591.

Sidler,M., Hassa,P., Hasan,S., Ringli,C. and Dudler,R. (1998) Involvement of an ABC transporter in a developmental pathway regulating hypocotyl cell elongation in the light. *Plant Cell*, **10**, 1623–1636.

Szczypka,M.S., Wemmis,J.A., Moye-Rowley,W.S. and Thiele,D.J. (1994) A yeast metal resistance protein similar to human cystic fibrosis transmembrane conductance regulator (CFTR) and multidrug resistance-associated protein. *J. Biol. Chem.*, **269**, 22853–22857.

Tam,Y.Y., Epstein,E. and Normanly,J. (2000) Characterization of auxin conjugates in *Arabidopsis*. Low steady-state levels of indole-3-acetyl-aspartate, indole-3-acetyl-glutamate and indole-3-acetyl-glucose. *Plant Physiol.*, **123**, 589–596.

Tommasini,R., Evers,R., Vogt,E., Mornet,C., Zaman,G.J.R., Schinkel,A.H., Borst,P. and Martinoia,E. (1996) The human multidrug resistance-associated protein functionally complements the yeast cadmium resistance factor 1. *Proc. Natl Acad. Sci. USA*, **93**, 6743–6748.

Tommasini,R., Vogt,E., Schmid,J., Fromentau,M., Amrhein,N. and Martinoia,E. (1997) Differential expression of genes coding for ABC transporters after treatment of *Arabidopsis thaliana* with xenobiotics. *FEBS Lett.*, **411**, 206–210.

Tommasini,R., Vogt,E., Fromentau,M., Hörtensteiner,S., Matile,P., Amrhein,N. and Martinoia,E. (1998) An ABC-transporter of *Arabidopsis thaliana* has both glutathione-conjugate and chlorophyll catabolite transport activity. *Plant J.*, **13**, 773–780.

Velten,J. and Schell,J. (1985) Selection-expression plasmid vectors for use in genetic transformation of higher plants.. *Nucleic Acids Res.*, **13**, 6981–6998.

Walker,J.E., Saraste,M., Runswick,M.J. and Gay,N.J. (1982) Distantly related sequences in the α- and β-subunits of ATP synthase, myosin, kinases and other ATP-requiring enzymes and a common nucleotide binding fold. *EMBO J.*, **1**, 945–951.

Winkler,R.G. and Feldmann,K.A.(1998) PCR-based identification of T-DNA insertion mutants. *Methods Mol. Biol.*, **82**, 129–136.

Received November 6, 2000; revised February 16, 2001; accepted February 20, 2001